Available online at www.sciencedirect.com
ScienceDirect
Polymer 48 (2007) 2755–2761
polymer
www.elsevier.com/locate/polymer

Effects of micelle structures formed in selective solvents on crystallization behaviors of poly(ethylene glycol)-*b*-poly(styrene) copolymers

Yan-Feng Chen [a], Feng-Bo Zhang [a], Xu-Ming Xie [a,*], Jin-Ying Yuan [b]

[a] *Advanced Materials Laboratory, Department of Chemical Engineering, Tsinghua University, Beijing 100084, China*
[b] *Department of Chemistry, Tsinghua University, Beijing 100084, China*

Received 10 August 2006; received in revised form 30 January 2007; accepted 6 March 2007
Available online 13 March 2007

Abstract

Well-defined amphiphilic block copolymers, poly(ethylene glycol) methyl ether-*b*-poly(styrene) (mPEG-*b*-PS), in which the PS blocks had different molecular weights, were synthesized by atom transfer radical polymerization (ATRP). Through introduction of selective solvents for the blocks, crystalline and amorphous blocks were self-assembled into different micelle structures in solutions. Atomic force microscopy (AFM) was used to characterize the micelle structures. It was observed that spherical micelles were always formed, whereas lamellar aggregates appeared only in the PS-selective solvent when the molecular weight of the PS block in mPEG-*b*-PS was low. The crystallizable mPEG blocks were self-assembled into either the core or corona of the micelles formed. The effects of the self-assembled structures on the crystallization behavior of mPEG blocks were then investigated with differential scanning calorimeter (DSC). When the PS molecular weight was much larger than that of mPEG, the result showed that the crystallinity of the mPEG block was lower when mPEG blocks crystallized in the corona than that in the core of the micelles. In this case, when mPEG blocks crystallized in micelle coronae, the micelle core formed by insoluble PS blocks was very big, so mPEG chains had to distribute sparsely in the micelle coronae. It was hard for mPEG chains in one micelle or among different micelles to gather together to crystallize. However, when the PS molecular weight was lower than that of mPEG, the crystallinity of mPEG was higher when the mPEG chains crystallized in the micelle corona, as the core formed by insoluble PS was small and the mPEG chains in the corona were easy to aggregate and crystallize.

Keywords: Poly(ethylene glycol)-*b*-poly(styrene); Micelle structure; Crystallization

1. Introduction

Block copolymers are composed of covalently linked chains of chemically distinct repeat units. Chemical distinction among different chains leads to ordered equilibrium mesophases, known as microphase separation. During the past years, it has been found that crystallization behaviors of crystalline block copolymers, i.e. melting temperature (T_m), crystallinity (X_c), crystal nucleation and growth, chain folding and orientation, are seriously influenced by microphase structures [1–16]. The most widely investigated systems are polyethylene-*b*-poly(vinyl cyclohexane) (PE-*b*-PVCH) [1–3], poly(ethylene oxide)-*b*-poly(butadiene) (PEO-*b*-PB) [4,5], polystyrene-*b*-poly(ethylene oxide) (PS-*b*-PEO) [6–9], poly(tetrahydrofuran)-*b*-poly(methyl methacrylate) (PTHF-*b*-PMMA) [10–12] and so on. Weimann et al. [1] showed that crystal nucleation and growth depended strongly on the type of microphase structures in PE-*b*-PVCH and PVCH-*b*-PE-*b*-PVCH systems. Chen et al. [5] studied the microdomain-tailored crystallization kinetics of PEO-*b*-PB, indicating that the crystallization temperature (T_c) dropped discontinuously when microphase structures transformed from lamellar, cylinder to sphere, although microdomains might be partially destroyed due to the crystallization process.

Furthermore, it is well known that in solvent, which is selective for one of the blocks, micelles usually formed when

* Corresponding author. Tel.: +86 10 62773607; fax: +86 10 62784550.
E-mail address: xxm-dce@mail.tsinghua.edu.cn (X.-M. Xie).

0032-3861/$ - see front matter © 2007 Elsevier Ltd. All rights reserved.
doi:10.1016/j.polymer.2007.03.023

solution concentration is well above the critical micelle concentration (cmc). Spherical micelles with a compact core of insoluble blocks surrounded by a corona of soluble blocks are most commonly seen. Besides, various novel self-assemblies, such as circular, interconnected tubules, and porous spheres, have been observed [17–26]. Micelle structures might be influenced by the crystallization behaviors of crystalline blocks. Gast and Cogan [17,18] explored the platelet aggregates formed by PS-*b*-PEO in cyclohexane with optical microscope (OPM) and transmission electron microscope (TEM). The platelet comprised a crystalline PEO layer between two brushes of swollen PS blocks. Recently, using atomic force microscope (AFM), Fu et al. [25] obtained well-developed lamellar micelles with insoluble poly(L-lactic acid) (PLLA) blocks folded to form crystal cores in PS-*b*-PLLA system.

In our previous work [27], it is proved that the confined and unconfined crystallization of crystalline block copolymers can be freely adjusted through controlling the competition between crystallization of crystalline block and vitrification of the amorphous block in solution. However, to date, systematical studies on crystallization behaviors of block copolymers, in particular with respect to self-assembly effect in solution, have been rarely reported. A better understanding on how crystallization behaviors were influenced by the self-assemblies prepared from selective solvents will be important and necessary.

In this paper, through use of selective solvents, crystalline and amorphous blocks are self-assembled into different micelle structures, with the crystalline blocks distributed either in the cores or in the coronae of the micelles. And then the effects of the self-assembly micelle structures on the crystallization behaviors of the copolymers are investigated.

2. Experimental part

2.1. Synthesis and characterization

The poly(ethylene glycol) methyl ether (mPEG) sample was from Fluka Chemika Co. ($\overline{M}_w$ = 5000, polydispersity (P_d) = 1.04, T_m = 58 °C). First the mPEG was endcapped with 2-bromopropionyl bromide (purchased from Aldrich) to yield functionalized macroinitiators mPEG-Br. The mPEG-Br was then used for atom transfer radical polymerization (ATRP) of styrene in bulk at 110 °C to synthesize the mPEG-*b*-PS with a molar ratio initiator/CuBr/2,2′-bipyridine of 1/1/3. The molecular weight of PS block was controlled by the polymerization time. Table 1 shows the $\overline{M}_w$ and P_d of the resulted mPEG-*b*-PS block copolymers, which were determined by JOEL JNM-ECA300 ^{1}H NMR and Viscotek TDA302 gel permeation chromatography (GPC) at room temperature, respectively.

Table 1
Characteristic data of block copolymers

Sample	$\overline{M}_w$ (copolymer)	$\overline{M}_w$ (PS)	P_d
EGS1	24 159	19 159	~1.24
EGS2	8490	3490	~1.04

2.2. Sample preparation

Each mPEG-*b*-PS sample was dissolved in toluene and $CHCl_3$/*n*-hexane (54/46 (v/v)) which are PS-selective and mPEG-selective, respectively. The concentration of all the solutions was fixed to be 0.005 g/ml. The solutions were kept for 2 days at room temperature for sufficient dissolution and micellization. The solutions were precipitated in a large excess of *n*-hexane. All the samples were then dried in a vacuum oven at room temperature to remove the residual precipitator fast. The *n*-hexane with a boiling point of 68.7 °C was easily removed in this way. By means of AFM, the precipitated micelle structures were observed. Then the crystallization behaviors of the micelles with different structures formed in selective solvents were investigated by DSC.

2.3. Atomic force microscopy

Tapping mode AFM imaging was performed on a Shimadzu SPM-9500J3 at room temperature. The AFM cantilever used was microfabricated from silicon and its spring constant and resonant frequency were 11.5 N m^{-1} and 255 kHz, respectively. Image analyses were performed using the corresponding commercial software.

2.4. Differential scanning calorimeter

The thermal analyses of mPEG-*b*-PS were performed at a rate of 10 °C/min with a Shimadzu TA-60WS DSC, which had been calibrated with standard indium and zinc before use. Each sample was heated from 0 °C to 60 °C as first run. After kept at 60 °C for 5 min, the sample was cooled down to −70 °C, and then heated to 70 °C again as second run. The X_c of each sample was calculated based on Eq. (1), with ΔH_m as the measured heat of fusion, $wt_{(mPEG)}$ as the weight percent of mPEG in the copolymer, and ΔH_m^0 as the theoretical heat of fusion of 100% crystalline poly(ethylene glycol), 188 J g^{-1} [28].

$$X_c = \frac{\Delta H_m}{wt_{(mPEG)}\Delta H_m^0} \times 100 \quad (1)$$

3. Results and discussion

3.1. Micelles prepared from selective solvents

Figs. 1 and 2 show AFM images of the micelle structures of EGS1 and EGS2 formed in different solvents, respectively. Spherical micelles are always formed, whereas lamellar aggregates appear only for EGS2 in the PS-selective solvent. The diameter of EGS1 spherical micelles formed in both PS- and mPEG-selective solvents is about 100 nm as shown in Fig. 1. For sample EGS2, spherical micelles formed in mPEG-selective solvent are about 60–70 nm in diameter, as given by the inset of Fig. 2(a). Because the molecular weight of the mPEG block is the same in EGS1 and EGS2, and the only difference between EGS1 and EGS2 is that the PS molecular weight of

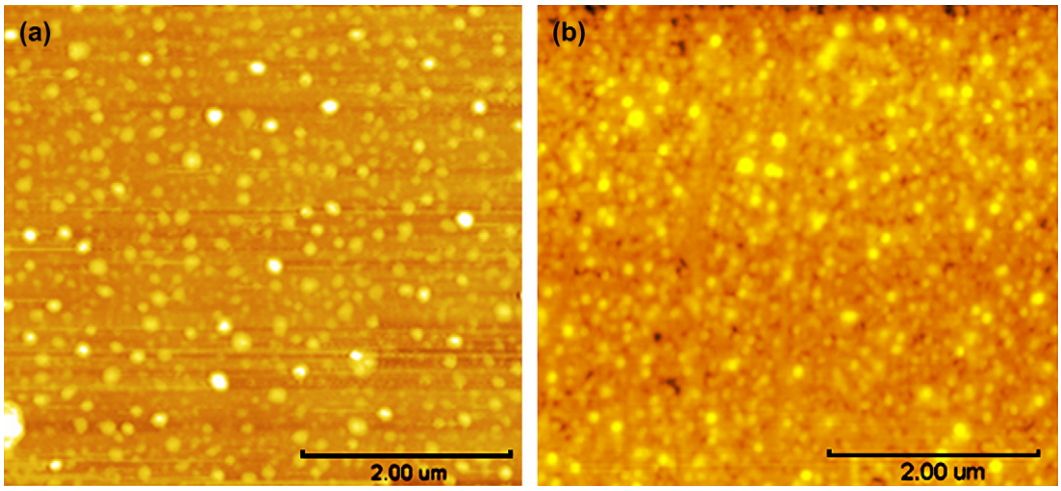

Fig. 1. AFM images of EGS1 micelles prepared from solvents (a) $CHCl_3$/*n*-hexane (mPEG-selective) and (b) toluene (PS-selective).

EGS2 is lower, the diameter difference may result from the difference of the molecular weight of the PS block. In other words, in mPEG-selective solvent, the insoluble PS core of EGS2 micelles was smaller than that of EGS1. Fig. 2(b) shows the AFM images of the lamellar aggregates formed in PS-selective solvent. Fig. 2(c) shows the corresponding spectra of the profile analysis along the lines A–B and C–D in Fig. 2(b). The lamellar micelles appeared as either single layer (A–B) or bilayer (C–D) with the layer thickness of about 10 nm. In this case, the PS molecular weight of the sample

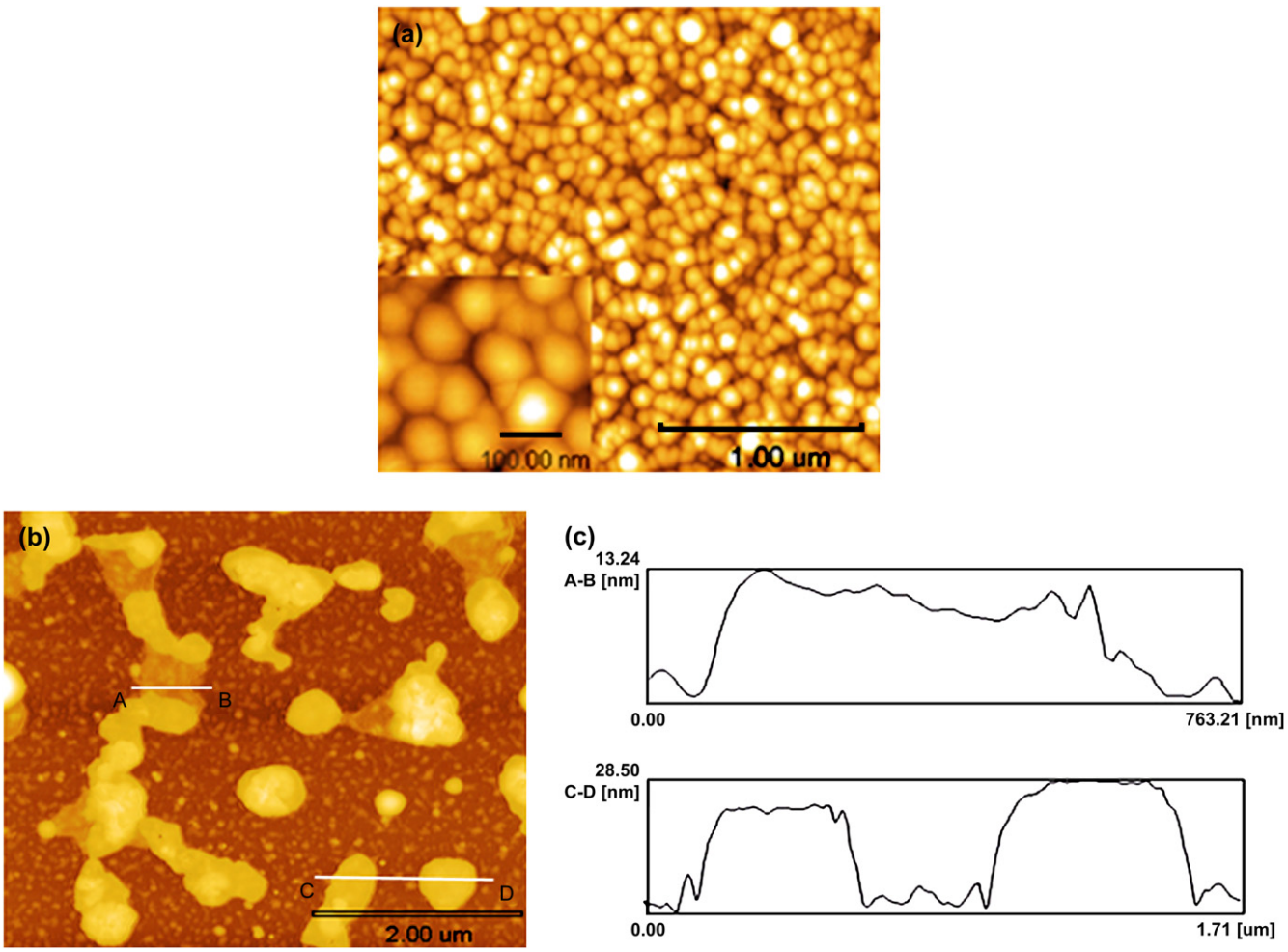

Fig. 2. AFM images of EGS2 micelles prepared from solvents (a) $CHCl_3$/*n*-hexane (mPEG-selective), the inset shows the higher resolution of micelles, (b) toluene (PS-selective); (c) is the profile analysis along the lines A–B and C–D in (b).

EGS2 is lower, so the crystallization of mPEG block in the core is preferred. The strong interactions among mPEG chains promoted a more ordered insoluble domain with less curvature, thus, lamellar micelles emerged instead of spherical micelles. It was considered that the lamella comprised a crystalline mPEG layer with soluble PS grafted on both sides [17,18,25].

3.2. Crystallization behaviors of EGS1

Fig. 3 shows the DSC curves of the EGS1 samples prepared from different selective solvents. In the first heating run as shown in Fig. 3(A), the melting temperature (T_m) of all the precipitated samples is about 53–54 °C. In the second heating run the T_m of all the samples becomes lower and the melting peaks are wider as shown in Fig. 3(A). When the EGS1 sample was prepared from the PS-selective solvent, the soluble PS chains in the corona of the micelle could move freely so the crystallization of insoluble mPEG chains in the core was not restricted. When the EGS1 sample was prepared from mPEG-selective solvent, the mPEG chains could move freely to crystallize. So the T_m in the first heating run was high in either selective solvents the samples were prepared from. Based on our previous papers [27,29,30], the crystallization process from the solutions is unconfined. In the second run, after the melting of the mPEG blocks, the block copolymer was kept at 60 °C, then cooled down to −70 °C and reheated again. According to Ref. [31], the glass transition temperature (T_g) of the PS block in the EGS1 sample was very high, nearly about 100 °C and higher than 60 °C, so during the second run of mPEG crystallization (the cooling process), the PS block was glassy and the micelle structures were retained. The mobility of mPEG chains linked with PS chains was restricted by the glassy PS and consequently the T_m became lower due to the confined crystallization. Similar results have been reported in other authors' and our previous papers [1,27,29,30]. Fig. 3(B) shows the crystallization temperature (T_c) of all the samples, which is very low, about −44 °C. The corresponding T_m, crystallinity X_c and T_c data of the EGS1 samples prepared from different selective solvents are all summarized in Table 2.

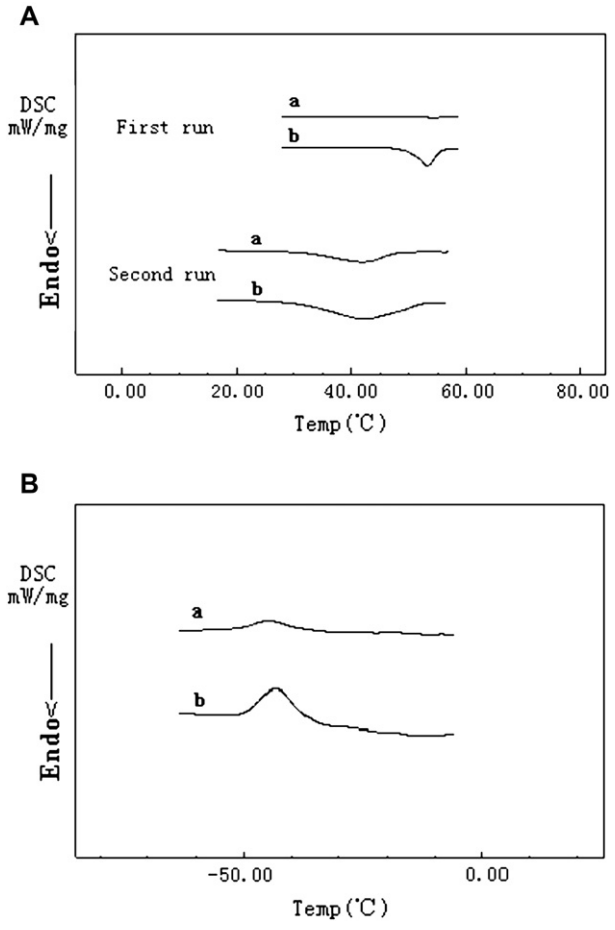

Fig. 3. DSC curves of the EGS1 sample prepared from different solvents (a) $CHCl_3$/*n*-hexane (mPEG-selective) and (b) toluene (PS-selective). (A) is the first and second heating run of DSC analysis and (B) is the curves of the mPEG crystallization in the second run.

As shown in Table 2, the X_c of the EGS1 sample prepared from the mPEG-selective solvent is much lower than that prepared from the PS-selective solvent in the first heating run. It implied that the micelle structures did have effects on mPEG crystallization. When prepared from the PS-selective solvent, the insoluble mPEG chains should be distributed in the micelle core with the soluble PS chains in the micelle corona. In this case, the mPEG blocks were aggregated and could crystallize easily. But when EGS1 was prepared from the mPEG-selective solvent, the soluble mPEG chains should be distributed in the micelle corona and the micelle core formed by the insoluble PS blocks was very big because the molecular weight of PS was much higher than that of mPEG for EGS1. Thus, the mPEG blocks had to distribute sparsely in the micelle corona. It was hard for mPEG chains in the same micelle or among different micelles to gather together to crystallize from solution, and the X_c was lower. However, after melting in the first run, the micelles were aggregated in the second process of mPEG crystallization. When mPEG blocks crystallized in the micelle corona from melt, there were more chances of the mPEG chains among different micelles to gather together to crystallize. Also, in the second run, during the cooling process from melt to −70 °C, the mPEG blocks could pass trough the T_c at −44.7 °C and crystallize sufficiently, so the X_c of mPEG increased for the EGS1 sample prepared from the mPEG-selective solvent. In other words, the crystallization of EGS1 in the first run was unconfined, but not complete. The increase in X_c of the EGS1 sample when the mPEG blocks crystallized in the micelle core in the second run could be explained only by the same cooling effect. Thus, the X_c of mPEG increased for all the EGS1 samples in the second run.

Table 2
Thermal analyses of the crystallization behaviors of EGS1

EGS1	Solvent	T_m (°C)	X_c (%)	T_c (°C)	Remark
a	$CHCl_3$/*n*-hexane	54.3	0.3	–	First run
	(mPEG-selective)	41.9	22.8	−44.7	Second run
b	Toluene	53.2	6.9	–	First run
	(PS-selective)	42.4	23.4	−43.3	Second run

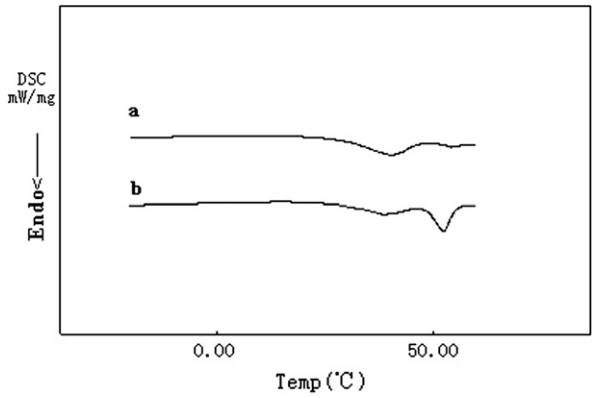

Fig. 4. DSC curves of the first heating run with the initial temperature at −70 °C for EGS1 samples. (a) $CHCl_3$/*n*-hexane (mPEG-selective) and (b) toluene (PS-selective).

In order to further verify our inferences for the crystallization and the X_c increase of mPEG in second run, the first heating run of DSC experiments was started from −70 °C, as shown in Fig. 4. Two peaks of T_m could be observed. The higher one was about 53 °C, which was the same with the heating process from 0 °C, as shown in Fig. 3(A). The lower T_m was about 42 °C, which did not appear in the heating process from 0 °C. It could be explained as follows. The higher T_m should be ascribed to the unconfined solution crystallization process. The solution crystallization process was not complete. During the cooling process to −70 °C, the mPEG chains could continue to crystallize. However, in this case the crystallization process was confined by the glassy PS and the T_m was lower. The corresponding confined T_m ($T_{m,con}$) and X_c ($X_{c,con}$), and unconfined T_m ($T_{m,un}$) and X_c ($X_{c,un}$) are shown in Table 3.

From Table 3, it was known that when the first heating process was started from −70 °C, the total X_c ($X_{c,con} + X_{c,un}$) was nearly the same in the first and second run for the sample treated with the PS-selective solvent, but for the sample treated with the mPEG-selective solvent the X_c was nearly doubled in the second heating run compared with the first. It could be concluded as follows: during the solution crystallization process, the micelles were generally separated to crystallize. However, after melting, the micelles could gather together to crystallize among different micelles, which contributed to the other half increase of the total X_c.

When the EGS1 samples prepared from selective solvents were heated to 110 °C, the resulted T_m and X_c of EGS1 were 43 °C and 28%, respectively. In this case, the micelle structures were destroyed because 110 °C was higher than the T_g of PS. Therefore during the cooling process the vitrification of PS happened before the crystallization of mPEG and mPEG has to crystallize in the separated microphase structures of the mPEG-*b*-PS copolymer. Either the mPEG block crystallized in the micelle structures is formed in solutions or microphase structures, the T_m of mPEG was almost the same. It implied that the chain end restriction was more important for T_m than the structure confinement [27,29,30].

As mentioned above, when the molecular weight of the PS block decreased, the structures of the micelles prepared from selective solvents were changed. The molecular weight effect of the PS block on the crystallization behavior of the mPEG block has to be further investigated.

Table 3
Thermal analyses of the crystallization behavior of samples

Sample	Solvent	$T_{m,un}$ (°C)	$T_{m,con}$ (°C)	$X_{c,un}$ (%)	$X_{c,con}$ (%)	Remark
a	$CHCl_3$/*n*-hexane (mPEG-selective)	54.1	40.2	0.5	10.9	First run
		–	41.9	–	22.8	Second run
b	Toluene (PS-selective)	52.1	38.6	9.3	10.3	First run
		–	42.4	–	23.4	Second run

3.3. Crystallization behaviors of EGS2

Fig. 5 shows the DSC curves of the EGS2 samples prepared from different selective solvents. As shown in Fig. 5(A), the T_m of all the samples is about 52 °C in the first run. In the second run, the T_m of all the samples is about 51 °C, which is nearly the same with the results of the first run. It meant that the constraint effect of the PS block on the mPEG crystallization was very weak, because the PS molecular weight of this sample was very low. The corresponding T_m and X_c data

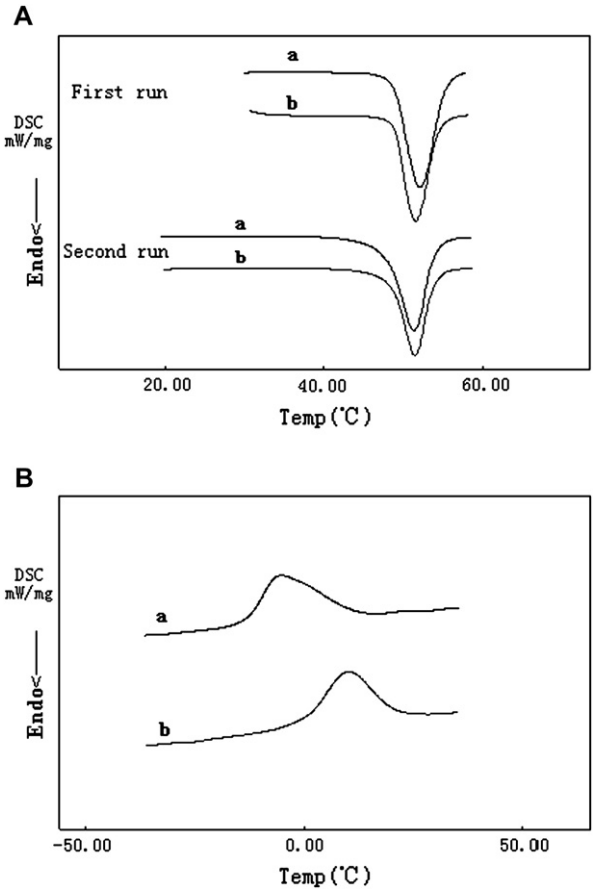

Fig. 5. DSC curves of sample EGS2 prepared from solvents (a) $CHCl_3$/*n*-hexane (mPEG-selective) and (b) toluene (PS-selective). (A) is the first and second heating run of DSC analysis and (B) is the cooling process of the second run.

Table 4
Crystallization behaviors of EGS2 prepared from different solvents

EGS2	Solvent	T_m (°C)	X_c (%)	T_c (°C)	Remark
a	$CHCl_3$/*n*-hexane	52.1	65.6	–	First run
	(mPEG-selective)	51.3	56.9	−5.3	Second run
b	Toluene	51.6	51.9	–	First run
	(PS-selective)	51.4	44.1	10.1	Second run

of the EGS2 samples prepared from different selective solvents are summarized in Table 4.

As shown in Table 4, the X_c of the EGS2 samples is much higher than that of EGS1 samples. It was due to the higher concentration of mPEG in the block copolymer and in the solution (the polymer concentration was fixed to be 0.005 g/ml in this work).

The X_c of EGS2 prepared from the mPEG-selective solvent was higher than that prepared from the PS-selective solvent in the first run, which was in contrast with EGS1. As mentioned above, in the mPEG-selective solvent, the insoluble PS core formed by EGS2 was smaller than that by EGS1 because of the lower PS molecular weight in EGS2. Hence, the distribution density of the mPEG chains in the micelle corona of EGS2 was higher than that of EGS1. Therefore, the aggregation possibility of mPEG chains from the same micelle or chains among different micelles increased and the X_c became high for the EGS2 sample. It was favorable for mPEG to crystallize in the micelle corona. However, when mPEG crystallized inside the lamellar aggregates which were prepared from the PS-selective solvent, the crystallization was slightly confined by the PS coronae grafted on the mPEG layer, so the X_c of EGS2 prepared from the PS-selective solvent was a little lower than that prepared from the mPEG-selective solvent in the first run.

Another difference between the EGS2 and EGS1 samples was that for EGS2 the X_c in the first run was higher than that in the second run whereas for the EGS1 sample the X_c in the second run was higher than that in the first run. When the EGS2 samples crystallized in solution, the less constraint of the PS block with lower molecular weight on relatively highly aggregated mPEG chains made the crystallinity X_c higher.

In addition, T_c of EGS2 micelles was higher than that of EGS1 micelles, implying that the sample of EGS2 could crystallize more easily and more completely.

It should be noticed that the T_c also varied with the solvents from which the samples were prepared from. The T_c of the samples, which were prepared from the mPEG- and PS-selective solvents was −5.3 °C and 10.1 °C, respectively. When the EGS2 sample was prepared from the PS-selective solvent, the mPEG chains were aggregated inside the lamellar aggregates. After the sample was melt and kept at 60 °C, the mPEG chains could still easily gather together to crystallize due to the retained micelle structure to a certain extent, so the crystallization occurred at a higher temperature. When the EGS2 sample was prepared from the mPEG-selective solvent, because the mPEG chains lay on the micelle corona, the aggregation of the mPEG chains was restricted by the hard PS core in the second process of mPEG crystallization. Thus, larger driving force was needed for crystallization and the T_c became lower.

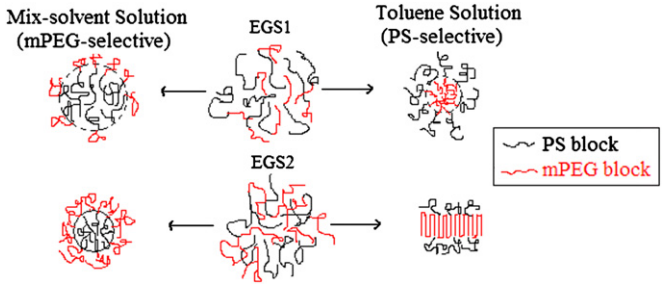

Fig. 6. Schematic drawing of the formation of the spherical and lamella micelles of EGS1 and EGS2 prepared from selective solvents.

The PS molecular weight of EGS2 was only 3500. As the T_g was molecular weight dependent, the T_g of this sample might be lower than 60 °C. However, the X_c and T_c difference indicated that the micelles formed had very good stabilities, and the heating process didn't destroy the micelle structures formed in solution, or at least the micelle structures were partially retained. Only when the temperature was risen to 100 °C, the micelle structures were destroyed and the T_cs were both about −9 °C.

A structure model was proposed for the micelle structures formed in solutions of the EGS1 and EGS2 samples as illustrated in Fig. 6. The spherical micelles were always formed except that the lamellar aggregates only formed in the PS-selective solvent for EGS2. The different diameters of the spherical micelles of EGS1 and EGS2 formed in the mPEG-selective solvent resulted from the different molecular weight of the PS block. In the mPEG-selective solvent, the insoluble PS core of EGS2 micelles was smaller and the distribution density of the soluble mPEG chains in the micelle corona was denser.

4. Conclusion

Various micelle structures were obtained from different selective solvents for mPEG-PS block copolymers. The micelle structures depended not only on the selective solvents, but also on the PS molecular weight. The crystallization behaviors of mPEG blocks, especially crystallinity, were strongly influenced by the micelle structures prepared from selective solvents. When the PS molecular weight was much larger than that of mPEG, the crystallinity of mPEG in the micelle core was lower than that in the micelle corona. In this case, the mPEG chains had to distribute sparsely in the micelle coronae due to the big micelle core of insoluble PS blocks. But when the molecular weight of PS was lower than that of mPEG, the core formed by insoluble PS was smaller and the mPEG chains in the corona were denser and easy to crystallize.

Acknowledgment

This project has been supported by a grant from the National Natural Science Foundation of China (Nos. 20674044, 10334020 and 50573036), which is gratefully acknowledged.

References

[1] Weimann PA, Hajduk DA, Chu C, Chaffin KA, Brodil JC. J Polym Sci B Polym Phys 1999;37:2053–68.
[2] Loo YL, Register RA, Adamson DH. Macromolecules 2000;33(22): 8361–6.
[3] Loo YL, Register RA, Ryan AJ, Dee GT. Macromolecules 2001;34(26): 8968–77.
[4] Zhu L, Calhoun BH, Ge Q, Quirk RP, Cheng SZD, Thomas EL, et al. Phys Rev B 1999;6:10022–31.
[5] Chen HL, Hsiao SC, Lin TL, Yamauchi K, Hasegawa H, Hashimoto T. Macromolecules 2001;34:671–4.
[6] Műller AJ, Balsamo V, Arnal ML, Jakob T, Schmalz H, Abetz V. Macromolecules 2002;35(8):3048–58.
[7] Zhu L, Cheng SZD, Calhoun BH, Ge Q, Quirk RP, Thomas EL, et al. J Am Chem Soc 2000;122(25):5957–67.
[8] Zhu L, Calhoun BH, Ge Q, Quirk RP, Cheng SZD, Thomas EL, et al. Macromolecules 2001;34(5):1244–51.
[9] Huang P, Zhu L, Guo Y, Ge Q, Jing AJ, Chen WY, et al. Macromolecules 2004;37(10):3689–98.
[10] Liu LZ, Jiang B, Zhou E. Polymer 1996;37:3937–43.
[11] Liu LZ, Yeh F, Chu B. Macromolecules 1996;29(16):5336–45.
[12] Liu LZ, Xu W, Li H, Su F, Zhou E. Macromolecules 1997;30(5): 1363–74.
[13] Hamley IW. Adv Polym Sci 1999;148:113–37.
[14] Hamley IW, Castelletto V, Floudas G, Schipper F. Macromolecules 2002; 35(23):8839–45.
[15] Opitz R, Lambreva DM, de Jeu WH. Macromolecules 2002;35(18): 6930–6.
[16] Shiomi T, Takeshita H, Kawaguchi H, Nagai M, Takenaka K, Miya M. Macromolecules 2002;35(21):8056–65.
[17] Cogan KA, Gast AP. Macromolecules 1990;23:745–53.
[18] Cogan-Farinas KA, Vinson PK, Gast AP. Macromolecules 1993;26: 1774–6.
[19] Yu K, Zhang LF, Eisenburg A. Langmuir 1996;12:5980–4.
[20] Yu K, Eisenburg A. Macromolecules 1996;29:6359–61.
[21] Zhang LF, Eisenberg A. J Am Chem Soc 1996;118:3168–81.
[22] Raez J, Manners I, Winnik MA. J Am Chem Soc 2000;122:11577–84.
[23] Raez J, Manners I, Winnik MA. J Am Chem Soc 2002;124: 10381–95.
[24] Raez J, Manners I, Winnik MA. Langmuir 2002;18:7229–39.
[25] Fu J, Luan B, Yu X, Cong Y, Li J, Pan CY, et al. Macromolecules 2004; 37:976–86.
[26] Wu J, Pearce EM, Kwei TK. Macromolecules 2002;35:1791–6.
[27] Yu PQ, Xie XM, Wang Z, Li HS. J Appl Polym Sci 2006;102(3):2584–9.
[28] Mandelkern L. J Appl Phys 1955;26:443–51.
[29] Yu PQ, Xie XM, Wang Z, Li HS. Polymer 2006;47(4):1460–4.
[30] Yu PQ, Xie XM, Wang Z, Li HS. Chem J Chin Univ 2005;3:583–5.
[31] Brandrup J, Immergut EH, Grulke EA. Polymer handbook. 4th ed. New York, NY: Wiley; 1999. p. V-92.